# Wigner distribution of amplitude and phase wide-band modulations in induction motor stator current

Baptiste Trajin, Jérémi Regnier, Jean Faucher, Marie Chabert

# Wigner distribution of amplitude and phase wide-band modulations in induction motor stator current

Baptiste TRAJIN, Jérémi REGNIER, Jean FAUCHER
Université de Toulouse; INP, UPS; LAPLACE; ENSEEIHT,
CNRS; LAPLACE;
2 rue Charles Camichel, BP 7122,
F-31071 Toulouse cedex 7
{baptiste.trajin, jeremi.regnier, jean.faucher}@laplace.univ-tlse.fr

Marie CHABERT
Université de Toulouse; INPT / ENSEEIHT - IRIT
2 rue Charles Camichel, BP 7122,
F-31071 Toulouse Cedex 7
marie.chabert@enseeiht.fr

**Abstract**

This paper deals with mechanical fault diagnosis in induction machines from stator current measurements. Mechanical faults lead to amplitude or phase modulations on stator currents that induce different time-frequency signatures. However, the time-frequency representations apply on complex signals for a univocal phase and modulus definition. When modulation frequencies are lower than the carrier frequency, this complex signal is the analytic signal obtained through the Hilbert transform of the real measured signal. However, bearing faults, for instance, may produce high frequency modulations. An alternative is to obtain the complex signal through the Concordia transform that takes advantage of the additional information available using two of the three phases of an electrical machine.
However, Concordia Transform requires the previous validation of a particular stator current model in three phase machine in case of mechanical faults. This paper uses the argument of the Fourier Transform for the validation of the model. Using the Hilbert and Concordia transforms of the proposed model, the Wigner-Ville distribution of narrow-band and wide-band frequency modulated signal is expressed. Finally, this paper applies the two transforms on simulated and experimental signals and provides a diagnosis of amplitude or phase modulation in various conditions.

**Keywords**
Induction Machine, Stator Current Analysis, Wide-band Modulations, Hilbert Transform, Concordia Transform, Wigner Distribution

## 1. Introduction

Monitoring techniques are intensively investigated to increase the reliability and safety of industrial systems using induction motors. Mechanical faults such as eccentricity and load

torque oscillations have been shown to produce respectively amplitude and phase modulation of the stator current [1]**.** The Wigner distribution allows to detect and classify the faults through their time-frequency signatures in steady state operation as well as at variable speed, and thus time-varying carrier frequency [2]. Through time-frequency analysis, the study of amplitude and phase modulations requires a rigorous definition of instantaneous amplitude and phase. For that purpose, a complex signal must be associated to the real measured one. The complex signal is classically obtained through the Hilbert transform of the real measured signal [3]. In case of wide-band modulations, the spectral or time-frequency signature can thus be misleading. As a contrary, using the Concordia transform, which is often used in electrical engineering for control purposes [4], a space vector can be built, that allows to diagnose amplitude and phase modulations [5].
This paper proposes a comparative study of the Wigner distribution derived from the Concordia space vector and the Hilbert analytic signal in steady-state and variable frequency applications. Section 2 presents and validates a stator current model in case of two elementary mechanical faults: airgap length variations and load torque oscillations. Section 3 recalls the Hilbert and Concordia transforms. Section 4 compares Wigner distributions obtained with the Hilbert analytic signal and Concordia space vector narrow and wide-band modulations using simulated and experimental stator currents. A diagnosis of amplitude or phase modulations is then provided.

## 2. Stator current model under mechanical faults

In three-phase machines, three current measurements with a phase separation of one-third cycle (120° or $2\pi/3$ rad) are available and can be written in the simple form:

$$i_k(t) = a(t)\cos\left(\psi(t) - \varphi_k\right), \text{ k=1,2,3} \tag{1}$$

The healthy machine is characterized by:

$$\begin{cases} a(t) = I \\ \psi(t) = 2\pi f_s t + \psi_0 \end{cases}$$

where $I$ denotes the stator current amplitude, $f_s$ the machine supply frequency and $\psi_0$ is the initial phase. Mechanical faults lead to particular expressions of $a(t)$ and $\psi(t)$. Airgap length variations and load torque oscillations are the main effects of mechanical faults [1]. They can be considered separately but a general default model involves their combination.

### *2.1 Amplitude modulations of stator currents*

In case of dynamic eccentricities (the center of the rotor turns around the geometrical stator center) or geometrical deformations of the rotor, the point of minimum airgap length is not stationary [6] The time varying airgap permeance causes an amplitude modulation (AM) of the stator current with carrier frequency $f_s$ such as [1]:

$$\begin{cases} a(t) = I\left[1 + \alpha\cos\left(2\pi f_{am} t + \varphi_{am}\right)\right] \\ \psi(t) = 2\pi f_s t + \psi_0 \end{cases} \tag{2}$$

where $\alpha$ denotes the AM index, $f_{am}$ the AM frequency and $\varphi_{am}$ the AM initial phase. One can notice that the AM caused by a geometrical deformation of the rotor may be such as $f_{am}>f_s$. In this situation, the dynamic eccentricity is said to cause wide-band AM.

### *2.2 Phase modulations of stator currents*

When submitted to periodic oscillations, the mechanical torque can be approached by the first term of its Fourier series decomposition:

$$\Gamma_{load}(t) = \Gamma_0 + \Gamma_c \cos\left(2\pi f_{pm} t\right) \tag{3}$$

where $\Gamma_c$ is the amplitude of the load torque oscillation and $f_{pm}$ the oscillation frequency. The stator current can be approached by a phase modulated (PM) signal [1], [7] such as:

$$\begin{cases} a(t) = I \\ \psi(t) = 2\pi f_s t + \beta \cos\left(2\pi f_{pm} t + \varphi_{pm}\right) + \psi_0 \end{cases} \tag{4}$$

where $f_{pm}$ is the PM frequency, $\varphi_{pm}$ is the PM phase, $\beta$ is the PM index function of $\Gamma_c$, $f_{pm}$ and $f_s$ [8]. In case of bearing or gear box faults for instance, the load torque oscillation frequency is a high multiple of the rotating frequency leading to wide-band PM of the measured stator current.

### *2.3 Signal model validation*

One can consider the general expression of the phase and/or amplitude modulated stator current (1), resulting from both airgap length variations and load torque oscillations. Using the Jacobi-Anger expansion [9] of $i_k(t)$ leads to:

$$i_k(t) = I\left[1 + \alpha \cos\left(2\pi f_{am} t + \varphi_{am}\right)\right] \sum_{n=-\infty}^{+\infty} J_n(\beta) \cos\left(2\pi f_s t + \psi_0 - \varphi_k + 2n\pi f_{pm} t + n\varphi_{pm}\right) \tag{5}$$

where $J_n(\beta)$ denotes the *n-th* order Bessel function of the first kind. For a very low index modulation ($\beta \approx 0$), the infinite sum can be approximated by the sum for $n \in \{-1,0,+1\}$. Moreover, the associated Fourier Transform (FT) of stator current $I_k(f)$ along the frequency $f$ is considered:

$$\begin{aligned} I_k(f) \approx & \frac{J_0(\beta)}{2} A(f) * \left[e^{j(\psi_0 - \varphi_k)} \delta\left(f - f_s\right) + e^{-j(\psi_0 - \varphi_k)} \delta\left(f + f_s\right)\right] \\ & + \frac{J_1(\beta)}{2} A(f) * \left[e^{j(\psi_0 - \varphi_k + \varphi_{pm})} \delta\left(f - f_s - f_{pm}\right) + e^{-j(\psi_0 - \varphi_k + \varphi_{pm})} \delta\left(f + f_s + f_{pm}\right)\right] \\ & + \frac{J_{-1}(\beta)}{2} A(f) * \left[e^{j(\psi_0 - \varphi_k - \varphi_{pm})} \delta\left(f - f_s + f_{pm}\right) + e^{-j(\psi_0 - \varphi_k - \varphi_{pm})} \delta\left(f + f_s - f_{pm}\right)\right] \end{aligned} \tag{6}$$

where * denotes the convolution product and with:

$$A(f) \approx I\delta(f) + \frac{\alpha I}{2}\left[e^{j\varphi_{am}}\delta(f - f_{am}) + e^{-j\varphi_{am}}\delta(f + f_{am})\right] \quad (7)$$

Finally, $I_k(f)$ is considered for $f=f_s+f_{pm}$ i.e. at the upper PM sideband component:

$$I_k(f_s + f_{pm}) = I\frac{J_1(\beta)}{2}e^{j(\psi_0 - \varphi_k + \varphi_{pm})} \quad (8)$$

The difference between consecutive argument values obtained for $k=1,2,3$ allows to check that the phase shift is $2\pi/3$. Then, the three stator currents have been measured on the induction machine in case of load torque oscillations. The supply frequency of the motor equals $f_s=50Hz$ and the load torque oscillation frequency equals $f_{pm}=21.2Hz$. Thus, the stator currents are phase modulated and the major harmonics set at $f_s-f_{pm}=28.8Hz$, $f_s=50Hz$ and $f_s+f_{pm}=71.2Hz$. The phase shift between each stator current component at $f_s+f_{pm}$ frequency is computed and compared to the theoretical value $2\pi/3$. The results are given in table 1.

**Table 1. Phase shifts between the three upper PM sideband components at $f_s+f_{pm}$ frequency**

| | Phase shift in rad | Absolute value of the relative error to $2\pi/3$ in % |
|---|---|---|
| $\lvert\varphi_2 - \varphi_1\rvert \bmod 2\pi$ | 2.088 | 0.27 |
| $\lvert\varphi_3 - \varphi_2\rvert \bmod 2\pi$ | 2.10 | 0.30 |
| $\lvert\varphi_1 - \varphi_3\rvert \bmod 2\pi$ | 2.106 | 0.57 |

These results provide a validation for the stator current model (1) in case of load torque oscillations. A similar analysis is achieved for stator currents in case of dynamic eccentricity and proves that the model in valid.

## 3. The need for a complex signal representation

The study of AM and/or PM requires the definition of the Instantaneous Amplitude (IA) and the Instantaneous Phase (IP). For a univocal definition, a complex signal has to be associated to the real observed signal [10]. Indeed, for a given real signal $x(t)$ there exists an infinite number of pairs $[A(t), \Psi(t)]$ such as $x(t)=A(t)\cos[\Psi(t)]$. The definition of IA and IP requires the construction of a canonical pair i.e. in one-to-one correspondence with $x(t)$.

### *3.1 Analytic signal via the Hilbert transform*

The classical way to define the IA and IP is to associate a complex signal to the measured real signal through the Hilbert Transform (HT). Let $X(f)$ denote the Fourier transform (FT) of $x(t)$. The analytic signal FT $X_{HT}(f)$ is given by [3]:

$$X_{HT}(f) = X(f) + jH(f)X(f) \text{ with: } H(f) = -j\,sign(f) \tag{9}$$

where:

$$sign(f) = \begin{cases} +1 \text{ for } f>0 \\ 0 \text{ for } f=0 \\ -1 \text{ for } f<0 \end{cases}$$

*H(f)* is the Hilbert filter transfer function. One can notice that the HT amounts to the cancellation of negative frequency components. When a modulation transfers significative components into the negative frequencies, the HT may yield misleading interpretations [11].

Indeed, the HT is submitted to the Bedrosian theorem conditions in case of modulated signals; the time-varying amplitude should have the characteristics of a low-pass signal whereas $cos[\Psi(t)]$ should be a high-pass signal [12]. Moreover, the bandwidth of $cos[\Psi(t)]$ has to be relatively small. Under the Bedrosian theorem conditions, the HT provides $A_{HT}(t)=a(t)$ as the IA and $\Psi_{HT}(t)=\Psi(t)$ as the IP. Thus, the IA (respectively IP) carries information about the AM (respectively the PM). Under Bedrosian theorem conditions, the HT allows to compute a component in quadrature with the real observed signal. One can notice that the PM is preferentially studied through the Instantaneous Frequency (IF) defined by:

$$IF(t) = \frac{1}{2\pi}\frac{d\Psi_{HT}(t)}{dt} \tag{10}$$

### *3.2 Space vector via the Concordia Transform*

In case of three-phase electrical machines, the three stator current measurements $i_1(t)$, $i_2(t)$ and $i_3(t)$ can be represented by a set of three coplanar vectors with a phase shift of $-2\pi/3$ rad. The CT is a linear transform which defines an orthogonal basis i.e. two components in quadrature $(i_\alpha, i_\beta)$ from the three previous vectors [4]. Assuming $\forall t$ , $i_1+i_2+i_3=0$, this linear transform can be expressed with the normalized Concordia matrix:

$$\begin{pmatrix} i_\alpha \\ i_\beta \end{pmatrix} = \sqrt{\frac{2}{3}} \begin{pmatrix} \sqrt{\frac{3}{2}} & 0 \\ \sqrt{\frac{1}{2}} & \frac{2}{\sqrt{2}} \end{pmatrix} \begin{pmatrix} i_1 \\ i_2 \end{pmatrix} \tag{11}$$

The complex space vector is defined by $i_{CT}(t)=i_\alpha(t)+j\, i_\beta(t)$. The CT is widely implemented in electrical drives for control purposes [4] and monitoring applications. For the three stator currents expressed according to (1), it can be easily shown from (11) that $i_{CT}(t)=a(t)e^{j\,\Psi(t)}$.

### *3.3 Comparison of Hilbert analytic signal and Concordia space vector*

The frequency contents of the IA and the IF obtained through HT and CT have been theoretically demonstrated in [5] for the stator in case of narrow-band and wide-band AM

and PM. The CT and HT provide the same complex signal when the Bedrosian theorem conditions are valid. However, when the Bedrosian theorem conditions are not valid, in case of wide-band modulations, extra harmonics appear in the IA and IF derived through HT. These extra harmonic may lead to a misleading diagnosis since AM appears as a PM and reciprocally. For this reason CT should be preferred to diagnose Am and PM on stator currents of a three-phase machine.

## 4. Application to time-frequency diagnosis through Wigner distribution

### *4.1 Definition*

The Wigner Distribution (WD) is a time-frequency energy distribution. The WD $W_z(t,f)$ of a complex signal $z(t)$ is defined as:

$$W_z(t,f) = \int_{-\infty}^{+\infty} z\left(t+\frac{\tau}{2}\right)\bar{z}\left(t-\frac{\tau}{2}\right)e^{j2\pi f\tau}d\tau \tag{12}$$

where $\bar{z}$ denotes the conjugate of z. The WD is the FT of the kernel $K_z(t,\tau)$ with respect to the delay variable $\tau$:

$$K_z(t,\tau) = z\left(t+\frac{\tau}{2}\right)\bar{z}\left(t-\frac{\tau}{2}\right) \tag{13}$$

The WD is of strong interest for detection and diagnosis purposes in electrical drives either in steady state or at variable speed. Indeed, contrarily to IA and IF spectra, the WD can be used in a non stationary context i.e. at variable speed or variable carrier frequency. Moreover, AM and PM (i.e. airgap length variations and load torque oscillations) can be distinguished from the phase analysis of the WD interference structure [1, 2]

### *4.2 Wigner distribution of steady state narrow-band PM and AM currents*

First a pure narrow-band PM with $\psi_0=0$ and $\varphi_{pm}=-\pi/2$ can be considered as a simplification. In case of narrow-band PM, the HT and CT complex signals are equal and such as:

$$i_{HT}(t) = i_{CT}(t) = Ie^{j\left(2\pi f_s t+\beta\sin\left(2\pi f_{pm}t\right)\right)} \tag{14}$$

Assuming $\beta<<1$, according to Bessel function properties, the associated WD can be derived using the Jacobi-Anger expansion:

$$W_{i_{HT}}(t,f) = W_{i_{CT}}(t,f) = I^2\left[\delta(f-f_s)+\beta\cos\left(2\pi f_{pm}t\right)\left[\delta\left(f-f_s-\frac{f_{pm}}{2}\right)-\delta\left(f-f_s+\frac{f_{pm}}{2}\right)\right]\right] \tag{15}$$

Thus the narrow-band PM current WD is characterized by a fundamental component at $f_s$ and periodic sidebands at $f_s \pm f_{pm}/2$ with frequency $f_{pm}$. One can notice that in case of PM, the sidebands are in phase opposition.
Now a pure narrow-band AM signal with $\psi_0 = \varphi_{am} = 0$ can be considered as a simplification. The HT and CT are such as:

$$i_{HT}(t) = i_{CT}(t) = I\left(1 + \alpha \cos\left(2\pi f_{am} t\right)\right) e^{j 2\pi f_s t} \tag{16}$$

Considering $\alpha << 1$, straightforward derivations lead to the associate WD:

$$W_{i_{HT}}(t, f) = W_{i_{CT}}(t, f) = I^2 \left[ \delta(f - f_s) + \alpha \cos\left(2\pi f_{am} t\right) \left[ \delta\left( f - f_s - \frac{f_{am}}{2} \right) + \delta\left( f - f_s + \frac{f_{am}}{2} \right) \right] \right] \tag{17}$$

The narrow-band AM WD is characterized by a fundamental component and periodic sidebands at frequencies at $f_s \pm f_{am}/2$ with frequency $f_{am}$ corresponding to the WD interference structure. One can notice that these components are in phase. The phase shift between interference terms can be used to distinguish narrow-band AM and PM.

### *4.3 Wigner distribution of steady state wide-band PM and AM currents*

According to section 3.3, in case of wide-band PM or AM, the diagnosis of modulation type cannot be performed. For instance, in the case of wide-band PM, the HT leads to an asymmetric interference structure with components at frequencies $f_s + f_{pm}/2$ and $f_{pm}/2$ and respective oscillating frequencies $f_{pm}$ and $2f_s - f_{pm}$:

$$W_{i_{HT}}(t, f) = I^2 \left[ \delta(f - f_s) + \beta \left[ \cos\left(2\pi f_{pm} t\right) \delta\left( f - f_s - \frac{f_{pm}}{2} \right) - \cos\left(2\pi (2 f_s - f_{pm}) t\right) \delta\left( f - \frac{f_{pm}}{2} \right) \right] \right] \tag{18}$$

A similar expression can be established for wide-band AM using the HT. The proposed diagnostic strategy, based on the phase shift between sideband interferences cannot be applied. On the contrary, CT leads to WD that express as (15) and (17) in case of pure wide-band PM and AM respectively. Then, the diagnosis of modulation type is allowed using the CT.

### *4.4 Experimental stator currents with load torque oscillations*

The experimental test bench is composed of a *5.5kW*, 2 pole pair induction machine supplied by a variable frequency Pulse Width Modulation inverter. The induction machine is coupled to a DC machine used as a mechanical load. The DC machine is connected to a resistor through a DC/DC converter which controls the DC motor armature current. The reference of the DC current is composed of an oscillating component at adjustable frequency plus an offset in order to induce load torque oscillations around a mean torque value. Experimental stator currents have been measured on the machine in two steady state conditions, where the supply frequency equals $f_s = 13.3Hz$ and then $f_s = 50Hz$ with a load torque oscillation of frequency $f_{pm} \approx 20Hz$. Thus, the stator currents are wide-band and

narrow-band PM signals. In Fig. 1(a) the WD is obtained through the HT analytic signal. In Fig. 1(b), the WD is computed using the CT space vector. In the narrow-band PM case, the two WD are similar with sideband components in phase opposition at frequencies $f_s \pm f_{pm}/2$. However, in the wide-band PM case, the WD derived from the HT analytic signals leads to a sideband component at frequencies $f_s + f_{pm}/2$ and $f_{pm}/2$, oscillating at frequency $f_{pm}$ and $2f_s - f_{pm}$ respectively. The WD derived from the CT space vector leads to sideband components at frequencies $f_s \pm f_{pm}/2$ in phase opposition. Consequently, as previously demonstrated, the CT allows to diagnose the narrow-band and wide-band PM in steady state conditions.

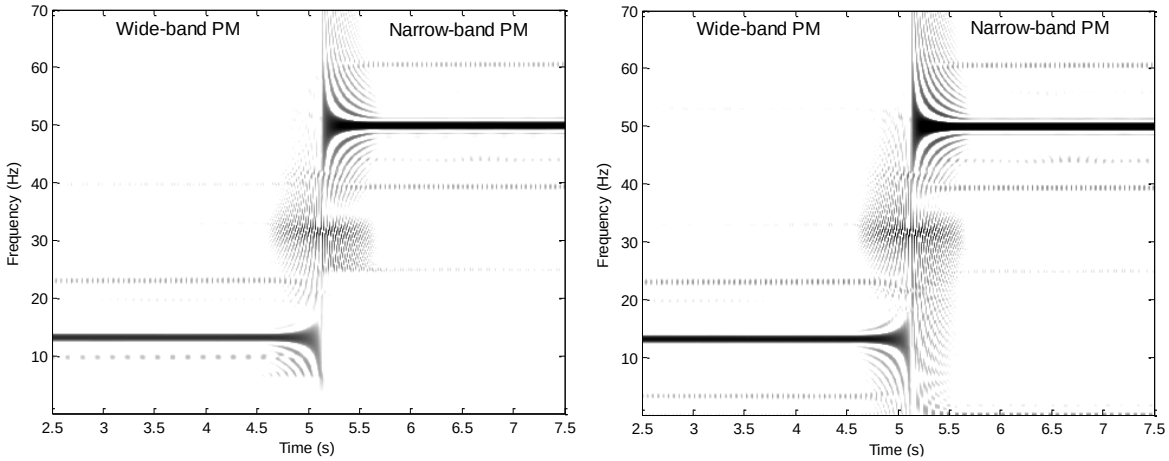


(a) WD from the HT analytic signal (b) WD from CT space vector

**Figure 1. WD computed using HT and CT for wide and narrow-band PM experimental currents in steady state**

### *4.5 Wigner distribution of stator currents at variable speed*

Finally, stator currents with variable supply frequency $f_s(t)$ and variable PM frequency $f_{pm}(t)$ are considered. Theoretical derivations have been performed in the particular case of a linear variation [2]. This case is studied through simulations only. The PM frequency equals $f_{pm}=1.4f_s$, consequently the Bedrosian theorem conditions are violated. As for steady state conditions, the WD computed from the CT space vector leads to sideband components at $f_s(t) \pm f_{pm}(t)/2$, in phase opposition whatever $f_s$. However, the WD obtained through the HT analytic signal leads to sideband components at frequencies $f_s(t) + f_{pm}(t)/2$ and $f_{pm}(t)/2$. One can notice that the two WD are similar in variable speed applications when the Bedrosian theorem conditions are satisfied. Fig. 2(a) displays the WD derived from the CT complex vector of the simulated PM stator current in this case. Fig. 2(b) provides a zoom on fundamental and interference components of the WD to ensure that sidebands are in phase opposition.

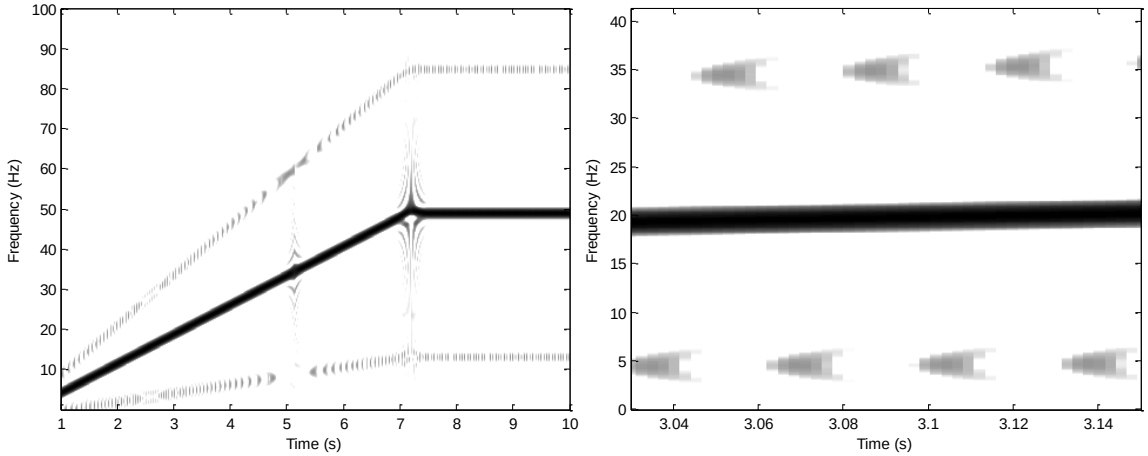


(a) WD from CT space vector (b) Zoom on sideband components

**Figure 2. WD from CT for simulated wide-band PM at variable speed**

## 5. Conclusions

Amplitude and phase modulation analysis through spectral or time frequency methods involves a complex signal for an univocal phase and amplitude definition. This paper has compared the Wigner distribution of complex signals obtained with the Hilbert and Concordia transforms in case of narrow and wide-band amplitude and phase modulations. This comparison is first conducted theoretically and then through simulated and experimental signals. The application to the time-frequency diagnosis based on Wigner distribution is developed. The Concordia transform provides an appropriate signal representation in the narrow and wide-band modulation cases. On the contrary, the Hilbert transform is limited by the Bedrosian theorem conditions to the analysis of narrow-band modulations. Phase and amplitude modulations, resulting from load torque oscillations and airgap length variations, can be detected and distinguished using the Wigner distribution of the complex signal. The Wigner distribution via Concordia transform provides a clear modulation diagnosis through the estimation of the phase shift between sideband components whatever the modulation frequency. As a consequence, when at least two stator current components are available, the Concordia transform should be preferred to build the complex signal required for the modulation analysis.

### References

[1] M. Blodt, J. Regnier and J. Faucher. “Distinguishing Load Torque Oscillations and Eccentricity Faults in Induction Motors Using Stator Current Wigner Distributions”, Industry Applications Conference, Vol. 3, pp. 1549-1556, Oct. 2006.

[2] M. Blodt, D. Bonacci, J. Regnier, M. Chabert and J. Faucher. “On-Line Monitoring of Mechanical Faults in Variable-Speed Induction Motor Drives Using the Wigner Distribution”, IEEE Transactions on Industrial Electronics, Vol. 55, n. 2, pp. 522-533, Feb. 2008.

[3] P. Flandrin. “Time-Frequency/Time-Scale Analysis” San Diego, Academic Press, 1999.

[4] P. Vas. “Electrical Machines and Drives – A space-vector theory approach”. Oxford Science Publications, Oxford, 1992.

[5] B. Trajin, M. Chabert, J. Regnier and J. Faucher. “Space vector analysis for the diagnosis of high frequency amplitude and phase modulations in induction motor stator current”. Condition Monitoring and Machinery Failure Prevention Technologies (CM2008/ MFPT2008), Edinbourgh, Jul. 2008.
[6] J.R. Cameron and W. T. Thomson. “Vibration and current monitoring for detecting airgap eccentricities in large induction motors”. IEE Proceedings, vol. 133, no.3, pp. 155--163, May 1986.
[7] M. Blodt, M. Chabert, J. Regnier and J. Faucher. “Mechanical Load Fault Detection in Induction Motors by Stator Current Time-Frequency Analysis”. IEEE Transactions on Industry Applications, Vol. 42, n. 6, pp. 1454-1463, Nov.-Dec. 2006.
[8] B. Trajin, J. Regnier, J. Faucher. “Bearing Fault Indicator in Induction Machine Using Stator Current Spectral Analysis”. Power Electronics Machine and Drives Conference, pp. 592-596, Apr. 2008.
[9] M. Abramowitz, I. A. Stegun. “Handbook of Mathematical Functions with Formulas, Graphs, and Mathematical Tables”. Dover Publications, New York, nineth ed., 1964.
[10] B. Picinbono. “On instantaneous amplitude and phase signal”. IEEE Transactions on signal processing, Vol. 45, n. 3, pp. 552-560, Mar. 1997.
[11] B. Boashash. “Estimating and interpreting the instantaneous frequency of a signal - Part 1 : Fundamentals”. Proceedings of the IEEE, Vol. 80, n. 4, pp. 520-538, Apr. 1992.
[12] E. Bedrosian. “A product theorem for Hilbert Transforms”. Proceedings of the IEEE, vol. 51, n° 5, pp. 868-869, May 1963.